Modeling and Control Strategy of a Single-Phase Uninterruptible Power Supply (UPS)

Dante Inga Narvaez, Marcelo Gradella Villalva
Department of Energy Systems (DSE), University of Campinas (UNICAMP)
Campinas, Brazil
dante.innar@gmail.com, marcelo@fee.unicamp.br

***Abstract*— The objective of this work is to get an understandable model of a single-phase Uninterruptible Power Supply (UPS), as well as design and verify the controllers for the UPS. To make the procedure more comprehensive, a basic single-phase UPS is proposed, so it is formed by a battery bank and a bidirectional full-bridge converter (with LC filter and transformer included). The single-phase full-bridge converter is modeled by deducing its transfer functions in two operational modes: voltage-controlled (stand-alone mode, to supply power to the load) and current-controlled (grid-tie mode, to charge the battery). Then, the controllers are designed by using the frequency-analysis approach, so the parameters of PI and PI+ressonant controllers are calculated as examples. External components such as the grid and the load are modeled in a simple way as well. The PSIM software is used to verify and compare the operation of the controllers through simulations, also being able to generate C code to implement the controller into a Digital Signal Processor (DSP). In addition, the models and controller design method can be re-utilized in simulations of other types of UPS and elements of a distributed microgrid.**

Keywords*— UPS, modeling, control, PI+ressonant, stand alone inverter, grid-tie inverter

I. INTRODUCTION

Since the last centuries, economic system in the world has become dependent on electric power, with the development of the industrial era, and the information era afterwards [1]. Modern systems require Uninterruptible Power Supplies (UPSs), especially for critical systems, in which classic diesel-based emergency generators are not fast enough to supply reliable and high-quality power for electronic loads or a microgrid.

II. UPS TYPES AND COMPONENTS

A. UPS Types

An UPS that uses static converters and an energy storage device, such as a battery or ultra-capacitor, is called a static UPS [2]. There are also rotating UPS systems, which use some rotating element such as a flywheel, and hybrid UPS, that are a combination of static and rotating. Static UPS systems are classified as on-line (the load is connected to the grid through the UPS, the storage device is fully charged), off-line (the load is connected directly to the grid, the storage device is fully charged and in stand-by mode), or line-interactive (the load and UPS are connected to the grid). Line-interactive UPS systems meet a good compromise between cost and performance. UPS can also be classified as single-phase or multi-phase (three-phase UPS is the most common).

B. UPS Components

An UPS is usually formed by an energy storage device, a bidirectional DC-DC converter, a bidirectional DC-AC inverter/rectifier, an output filter and a static transfer switch [3].

Modeling, sizing and control of UPS are found in the literature mainly for the three-phase UPS [4-10], and for single-phase also, but explained in a difficult way or not in detail [11-15].

III. MODELING, SIZING AND CONTROL

A basic single-phase UPS is proposed, as it is shown in Fig. 1., in order to develop an understandable procedure of modeling, sizing and control. This UPS has the fundamental parts: battery bank V_{bat} and full-bridge bidirectional converter (transistors *T1-4*, with LC filter and transformer *TX*). External components such as load *R* and grid voltage V_{grid} are also represented. The ideal switch *S* simulates a grid fault by disconnecting the grid from the load. There are two operating modes: voltage-controlled (the grid is out, so the system supplies power to the load, if the battery is charged) and current-controlled (the grid is present, so the system charges the battery bank, or keeps it charged).

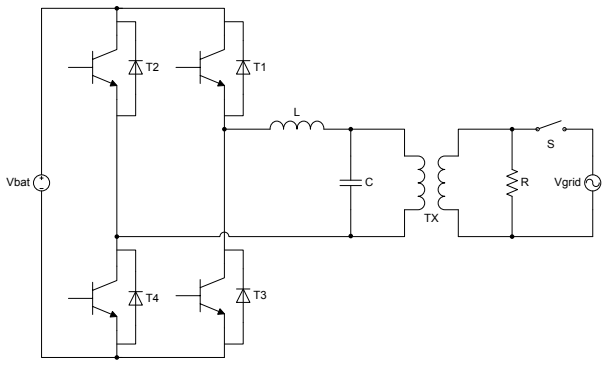

Fig. 1. Schematic diagram of a basic single-phase UPS.

978-1-4673-6605-2/15/$31.00 ©2015 IEEE

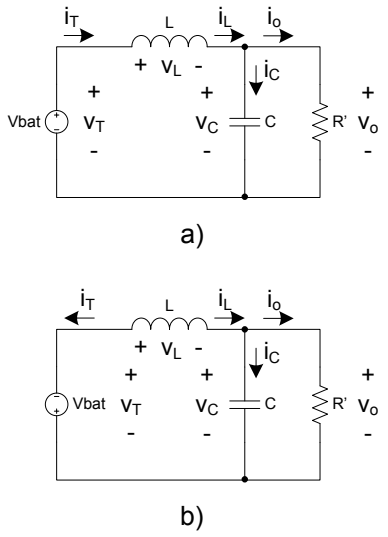

Fig. 2. Equivalent circuits for a) d interval and b) d' interval.

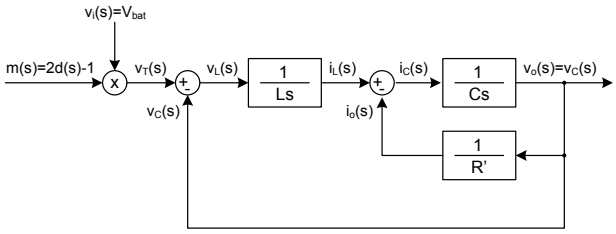

Fig. 3. Block diagram of the full-bridge converter.

A. Full-Bridge Converter Modeling

The full-bridge converter is one of the most used converters as inverter, rectifier, or bidirectional converter. The schematic diagram of this converter is shown in Fig. 2. Initially, to simplify the analysis, the battery bank is modeled as a DC source V_{bat}, and the load is modeled as an equivalent resistor R'. The model obtained is also valid for the single-phase UPS, as it will be shown.

From Fig. 2, applying Ohm's laws for inductor voltage and capacitor current, taking into account the physical laws for the passive components R', L and C:

$$\begin{cases} v_L = L\frac{d}{dt}i_L = v_T - v_o = v_T - v_C \\ i_C = C\frac{d}{dt}v_C = i_L - i_o = i_L - \frac{1}{R'}v_C \end{cases} \quad (1)$$

If the converter is driven by a PWM modulator (d is the duty cycle and d' is its complementary signal) and the converter is in steady-state operation, two equivalent circuits will be obtained (during every dT_s and $d'T_s$ time intervals, where T_s is the switching period). Equivalent circuits for both time intervals d and d' are shown in Fig. 3. During the first interval d, T1 and T4 are closed (T2 and T3 are open), so the input source is connected in the same polarity compared to the output voltage.

$$d: \begin{cases} v_L = L\frac{d}{dt}i_L = V_{bat} - v_C \rightarrow v_T = V_{bat} \\ i_C = C\frac{d}{dt}v_C = i_L - \frac{1}{R'}v_C \end{cases} \quad (2)$$

During the second interval $d'=1-d$, T2 and T3 are closed (T1 and T4 are open), so the input source is connected in opposite polarity compared to the output voltage.

$$d': \begin{cases} v_L = L\frac{d}{dt}i_L = -V_{bat} - v_C \rightarrow v_T = -V_{bat} \\ i_C = C\frac{d}{dt}v_C = i_L - \frac{1}{R'}v_C \end{cases} \quad (3)$$

Averaging the equations (2) and (3) for steady-state operation, for time intervals d and (1-d) respectively:

$$\begin{cases} v_L = V_{bat}d - V_{bat}(1-d) - v_C = (2d-1)V_{bat} - v_C \\ i_C = i_L - \frac{1}{R'}v_C \end{cases} \quad (4)$$

Defining the modulation index as $m=2d-1$:

$$\begin{cases} v_L = L\frac{d}{dt}i_L = mV_{bat} - v_C \\ i_C = C\frac{d}{dt}v_C = i_L - \frac{1}{R'}v_C \end{cases} \quad (5)$$

By comparing equations (5) and (1) it is possible to find the averaged value of signal v_T (in a similar way for i_T):

$$\begin{cases} v_T = mV_{bat} \\ i_T = i_L d - i_L(1-d) = mi_L \end{cases} \quad (6)$$

Applying the Laplace transformation to equation (5) to get the dynamics:

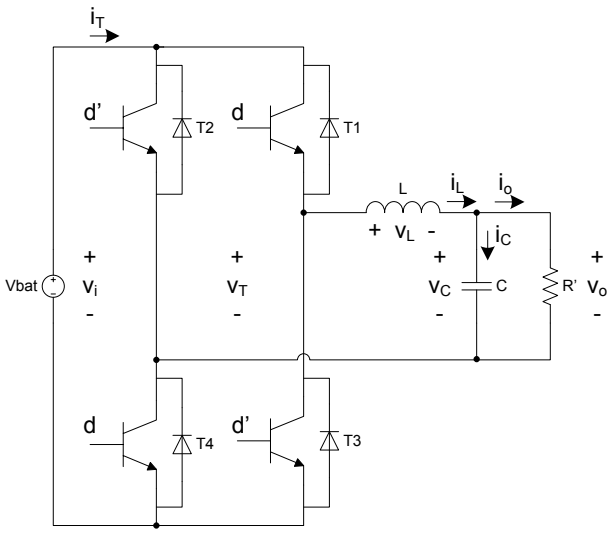

Fig. 4. Equivalent circuit for the full-bridge converter.

$$\begin{cases} v_L(s) = (Ls)i_L(s) = m(s)V_{bat} - v_C(s) \\ i_C(s) = (Cs)v_C(s) = i_L(s) - \frac{1}{R'}v_C(s) \end{cases} \quad (7)$$

The block diagram of the full-bridge converter can be constructed from the equations (7) and (1), as it can be seen in Fig. 4. Transfer functions can be deduced from the diagram:

$$(Cs)v_C = i_L - \frac{1}{R'}v_C \rightarrow \frac{v_C(s)}{i_L(s)} = \frac{\frac{1}{C}}{s + \frac{1}{R'C}}$$

$$(Ls)i_L = mV_{bat} - v_C \rightarrow \frac{i_L(s)}{m(s)} = \frac{\frac{V_{bat}}{L}(s + \frac{1}{R'C})}{s^2 + \frac{1}{R'C}s + \frac{1}{LC}} \quad (8)$$

$$\frac{v_C}{m} = \frac{v_C}{i_L} \cdot \frac{i_L}{m} \rightarrow \frac{v_C(s)}{m(s)} = \frac{\frac{V_{bat}}{LC}}{s^2 + \frac{1}{R'C}s + \frac{1}{LC}}$$

B. *Sizing of the System*

The parameters of the full-bridge converter are set or calculated, and they depend on the sizing of the system [16]. If the battery bank is formed by five 12 V lead-acid batteries connected in series, and the maximum value of modulation index is m=0.5: V_{bat} = 5 x 12 = 60 V, $v_{C(peak)} = m\ V_{bat}$ = 30 V. For a 180 V(peak) grid system, a voltage-elevator transformer with turns-ratio N=6 is needed. Besides that, for an output power P_o=90W: $v_{grid(peak)} = N\ v_{C(peak)}$ = 180 V; $R = v^2_{grid(peak)}/(2P_o)$ = 180 Ω; $R' = R/N^2$ = 5 Ω.

As full-bridge converter behaves like a buck converter in inverter mode, except for the fact that the modulation index m (and the duty cycle d as well) varies in a sinusoidal way, maximum values of duty cycle d and current ripple factor CRF determine the value of the inductance L (switching frequency is f_s=15kHz):

$$m_{\max} = 0.5 \rightarrow d_{\max} = \frac{m_{\max} + 1}{2} = 0.75$$

$$CRF_{\max} = 1.67\% \rightarrow L = \frac{R'(1 - d_{\max})}{f_s CRF_{\max}} = 5mH$$

The value of capacitance can be determined by the cut frequency f_f of the passive filter (it has to be much greater than the modulating frequency f_m, but much less than the switching frequency f_s), and it determines the voltage ripple factor VRF:

$$f_f = 710Hz \rightarrow C = \frac{1}{(2\pi f_f)^2 L} = 10uF$$

$$f_s = 15kHz \rightarrow VRF_{\max} = \frac{1 - d_{\max}}{8 f_s{}^2 LC} = 0.28\%$$

C. *Voltage-Controlled Mode*

If a grid outage occurs, the UPS must supply power to the load, so an output voltage controller is needed. In this case, input voltage is DC (V_{bat}=60V), battery resistance is neglected (R_{bat}=0.5Ω), and modulation index $m(t)$ is sinusoidal in order to get a sinusoidal output voltage $v_o(t)$.

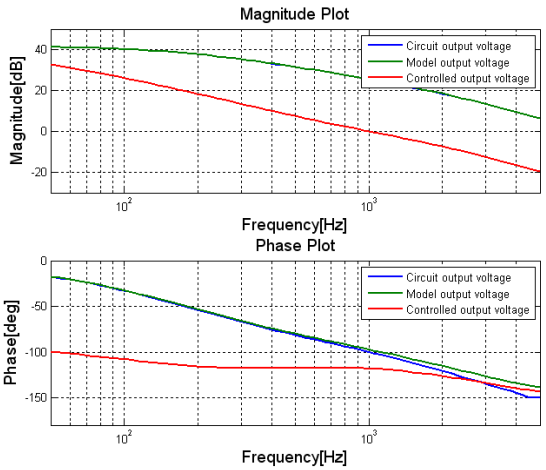

Fig. 5. Bode plots of circuit, model and controlled output voltage.

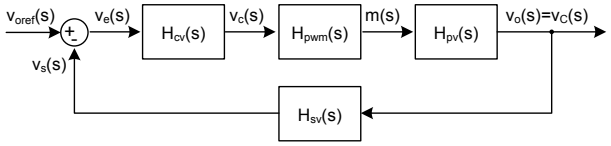

Fig. 6. Full-bridge converter model with output voltage control.

Control loop is shown in Fig. 5. Bode diagrams of $H_{pv}(s)$ are calculated and verified with PSIM, in order to get the gain and phase of the plant at the desired cut frequency (f_c=1 kHz):

$$H_{pv}(s) = \frac{v_C(s)}{m(s)} = \frac{1.20\times10^9}{s^2+2.00\times10^4 s+2.00\times10^7}$$

The frequency analysis approach can be used to design many controllers. PI controller is designed as a first example:

$$H_{cv}(s) = k_p + \frac{k_i}{s} = \frac{k_p(s + \frac{k_i}{k_p})}{s}$$

To meet stability condition, unity open-loop gain and phase margin have to be satisfied at the desired cut frequency. For example, if phase margin PM=60º, modulator gain H_{pwm}=1/V_s=1/1.5 and sensor gain H_{sv}=1/30

$$H_{olv} = H_{cv}H_{pwm}H_{pv}H_{sv} = \frac{4\times10^7 k_p(s + \frac{k_i}{k_p})}{1.5s(s^2 + 2\times10^4 s + 2\times10^7)}$$

$$\begin{cases} \text{Phase}(H_{olv}) = -180° + 60° \rightarrow \frac{k_p}{k_i} = 4.12\times10^{-4} \\ \text{Gain}(H_{olv}) = 1 \rightarrow k_p = 4.45, k_i = 1.08\times10^4 \end{cases}$$

Bode diagrams of magnitude (at the top) and phase (at the bottom) can be observed in Fig. 6, for the output voltage of the simulated circuit (blue), modeled circuit (green) and controlled loop (red). It is verified that the circuit and the model have very close Bode diagrams, and open-loop circuit meets the requirements of amplitude (0dB) and phase (-120°).

The PI+resonant controller can be designed by using the parameters of the PI controller just calculated (f_m=60Hz):

$$H_{cv}(s)=\frac{k_p(s^2+2\frac{k_i}{k_p}+w_m{}^2)}{s^2+w_m{}^2}$$

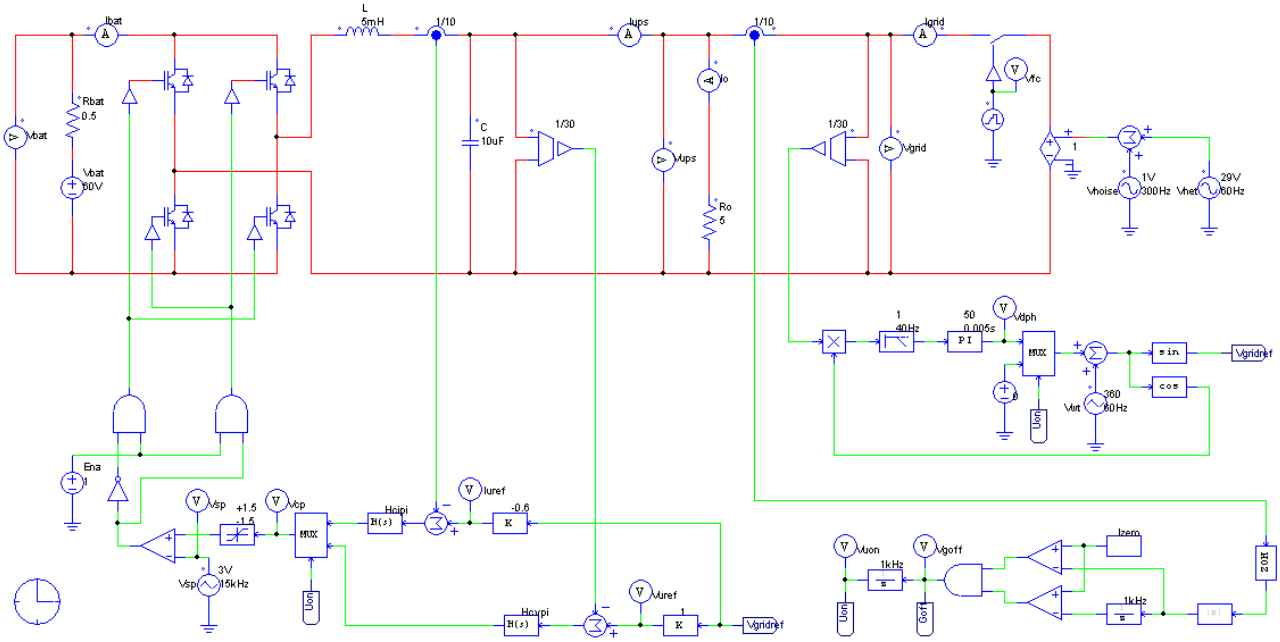

Fig. 7. Complete system with voltage an current loop controllers simulated with PSIM.

D. *Current-Controlled Mode*

In this mode the grid is present, so it is also connected to the output of the converter in parallel to the load, and the battery is connected to the converter input. Therefore, to charge the battery, an inductor current controller is needed. Grid current is considered as a disturbance for the model, so the transfer function is the same as in the initial case.

$$H_{pi}(s)=\frac{i_L(s)}{m(s)}=\frac{1.20\times10^4(s+2.00\times10^4)}{s^2+2.00\times10^4 s+2.00\times10^7}$$

A similar procedure is followed to calculate the parameters of the current controller. Given a PI controller as an example, if the cut frequency f_c = 1 kHz and phase margin PM=60º (H_{pwm}=1/1.5, H_{si}=1/10):

$$H_{oli}=H_{ci}H_{pwm}H_{pi}H_{si}=\frac{800k_p(s+2\times10^4)(s+\frac{k_i}{k_p})}{s(s^2+2\times10^4 s+2\times10^7)}$$

$$\begin{cases}Phase(H_{oli})=-180°+60°\rightarrow\frac{k_p}{k_i}=1.99\times10^{-4}\\ Gain(H_{oli})=1\rightarrow k_p=5.93, k_i=2.98\times10^4\end{cases}$$

Then, PI current controller is specified as:

$$H_{ci}(s)=\frac{k_p(s+\frac{k_i}{k_p})}{s}=\frac{5.93(s+5.02\times10^3)}{s}$$

The PI+resonant controller can be specified as well:

$$H_{ci}(s)=\frac{5.93(s+10^4 s+1.52\times10^4)}{s^2+1.52\times10^4}$$

E. *Battery Bank and Grid Modeling*

In this work the battery bank is modeled as a simple DC voltage source in series with a series resistance. This model will be improved in the future with experimental data.

The grid voltage source is simulated in PSIM with a simple sinusoidal voltage source. Distortion can be modeled as another sinusoidal voltage source with smaller amplitude and higher frequency, which is added to the grid voltage and coupled to the power circuit.

Grid-fault event is simulated by using a bidirectional switch, a gate driver, and a pattern generator source to control the period of time in which the grid voltage will be available. In that case, the converter transfer function changes, and the supervisory controller has to change the controller as well.

F. *The Supervisory Controller*

The supervisory controller uses a Zero-Current Detector (ZCD) to sense a grid fault, and a Phase-Locked Loop (PLL)

to determine instantaneous grid phase. Thus, it generates reference signals for voltage and current controllers, as well as control signals for multiplexer (MUX) and PWM modulator. The block diagram of the supervisory controller is shown in Fig. 7.

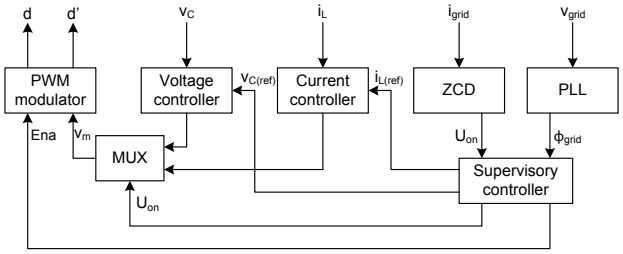

Fig. 8. Block diagram of the system controller.

IV. Simulation Results

A. Full-Bridge Converter as an Inverter

The schematic diagram of the complete system with output voltage and current controllers is shown in Fig. 8. In the stand-alone mode, as battery maintains the input voltage almost constant, only one PI controller is enough to guarantee that the output voltage will follow the reference signal. Two types of controllers were simulated (see Fig. 9a). It can be noticed that the error in the output voltage with PI+resonant controller (green) is verified to be less than the error in output voltage with PI controller (blue). In addition, more sophisticated controller techniques can be tested, such as repetitive, adaptive or fuzzy-based controllers.

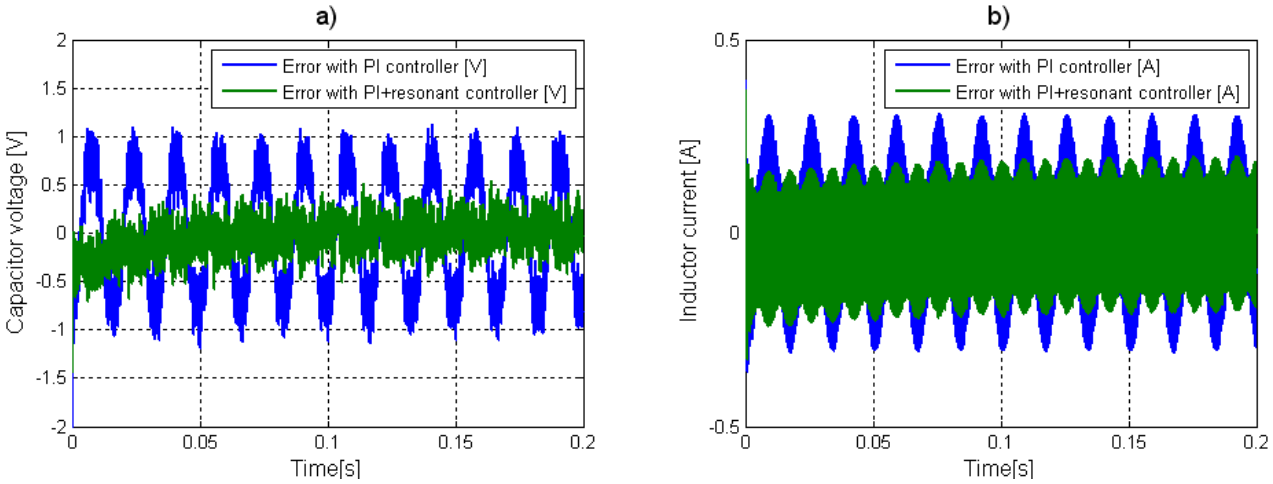

Fig. 9. Simulation of a) voltage control and b) current control in the full-bridge converter, with PI and PI+resonant controllers.

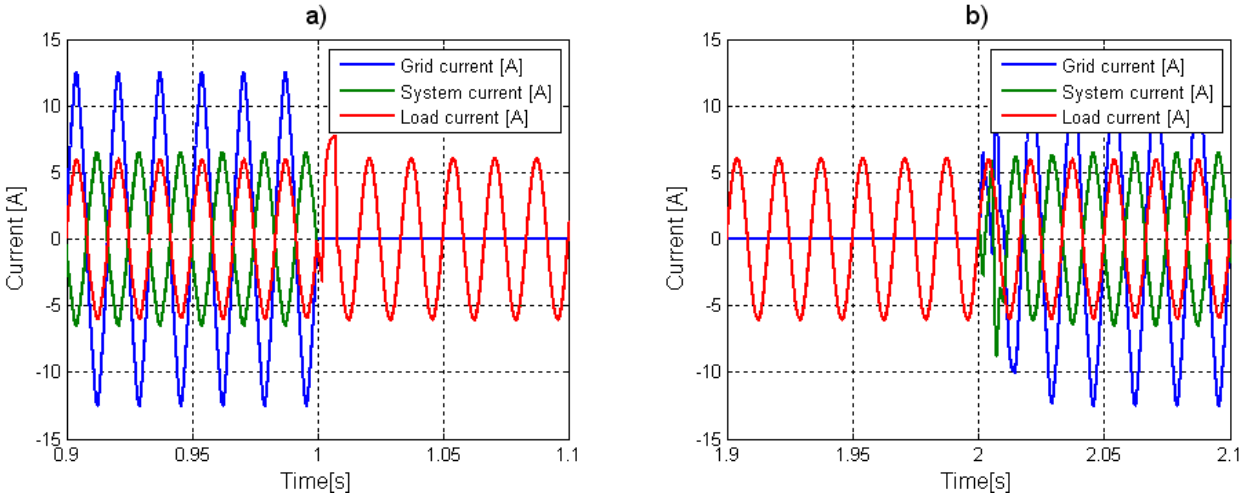

Fig. 10. Simulation of a) grid outage and b) reconnection events managed by the UPS.

B. *Full-Bridge Converter as a Rectifier*

In the grid-connected case, the battery maintains the DC input voltage constant, and the grid maintains the AC output voltage as sinusoidal. Therefore only one PI controller is needed to keep the inductor current sinusoidal, as it is verified in Fig. 9b. As the reference signal is negative, the reverse current flow charges the battery from the grid. It is also verified that the error in the inductor current with PI+resonant controller (green) is less than the error in inductor current with PI controller (blue).

C. *Grid Outage and Reconnection Events*

Fig. 10 presents simulations of currents at grid outage (Fig. 10a) and grid reconnection (Fig. 10b) events. The supervisory controller uses a zero current detector to track a grid outage, and enables the voltage controller in order to supply power to the load. In the presence of an outage event, the grid current (blue) goes to zero. It is verified that the UPS current (green) changes its polarity, while the load current (red) is maintained. Transients observed can be reduced by improving the supervisory control, by providing the proper delays to the control and enable signals.

V. CONCLUSIONS

A single-phase, full-bridge based UPS was modeled in a comprehensive way, and controllers were designed by frequency domain analysis and verified by simulations with PSIM.

The model can be extended by adding a DC-DC converter between the battery and the full-bridge converter. Therefore, one additional control loop for each operating mode will be needed, and other types of controllers can be tested. In addition, grid islanding will be implemented in future research.

The designed UPS can be integrated into more complex simulations, such as a distributed generating system for a microgrid.

ACKNOWLEDGMENT

This work was supported by CNPq (454352/2014-0), PAPDIC/PRP/UNICAMP, and CAPES/PROEX.

REFERENCES

[1] P. M. Curtis, “Maintaining Mission Critical Systems in a 24/7 Environment”, 2011.

[2] P. J. Grbovic, “Ultra-Capacitors in Power Conversion Systems: Applications, Analysis and Design from Theory to Practice”, 2014.

[3] S. M. Sharkh, M. A. Abusara, G. I. Orfanoudakis and B. Hussain, “Power Electronic Converters for Microgrids”, 2014.

[4] A. I. Maswood, J. E. Al-Ammar, “Analysis of a PWM Voltage Source Inverter with PI Controller under Non-ideal conditions”, 2010.

[5] L. Xiao-xian, W. Wei-nong, Z. Lei, D. Ya-Ii, “Study on novel fuzzy controller and its application in PWM inverters”, 2012.

[6] C. T. Ri , N. S. Choi, G. C . Cho, G. H . Cho, “A Complete DC and AC Analysis of Three Phase Current Source PWM Rectifier Using Circuit DQ Transformation”, 1992.

[7] H. Soo-bin, C. Nam-sup, R. Chun-tak, C. Gyu-hyeong, “Modeling and Analysis of Buck Type Three Phase PWM Rectifier by Circuit DQ Transformation”, 1995.

[8] H. Mao, D. Boroyevich, F. C. Y. Lee, “Novel Reduced-Order Small-Signal Model of a Three-Phase PWM Rectifier and Its Application in Control Design and System Analysis”, 1998.

[9] B. Yin, R. Oruganti, S. K. Panda, A. K. S. Bhat, “Experimental Verification of a Dual Single-Input Single-Output Model of a Three-Phase Boost-Type PWM Rectifier”, 2005.

[10] T. S. Lee, J. H. Liu, “Modeling and Control of a Three-Phase Four-Switch PWM Voltage-Source Rectifier in d-q Synchronous Frame”, 2011.

[11] J. Lee, G. Park, J. Choi, “CRA Based Robust Digital Controller for a Single Phase UPS Inverter”, 2007.

[12] T. Saigusa, K. Imamura, T. Yokoyama, “100kHz Single Phase Utility Interactive Inverter with FPGA based Hardware Controller”, 2010.

[13] Z. Guo, S. Kurokawa, “A Novel PWM Modulation and Hybrid Control Scheme for Grid-connected Unipolar Inverters”, 2011.

[14] S. M. Cherati, N. A. Azli, S. M. Ayob, A. Mortezaei, “Design of a Current Mode PI Controller for a Single-phase PWM Inverter”, 2011.

[15] M. Gonzalez, V. Cardenas, F. Pazos, “DQ Transformation Development for Single-Phase Systems to Compensate Hannonic Distortion and Reactive Power”, 2004.

[16] D. I. Brandão, “Sistema de Geração Fotovoltaico Multifuncional”, Master Thesis, UNESP, 2013.